



Cite this: *J. Mater. Chem. B*,
2024, 12, 9144

Received 26th April 2024,
Accepted 29th July 2024

DOI: 10.1039/d4tb00900b

rsc.li/materials-b

A novel method for the diagnosis of atherosclerosis based on nanotechnology

Ying Yang,^{ab} Jiangpeng Pan,^{ab} Aifeng Wang,^{ab} Yongcheng Ma,^{ab} Ying Liu^{*ab} and Wei Jiang ^{*ab}

Cardiovascular disease (CVD) is a global health concern, presenting significant risks to human health. Atherosclerosis is among the most prevalent CVD, impacting the medium and large arteries in the kidneys, brain, heart, and other vital organs, as well as the lower limbs. As the disease progresses, arterial obstruction can result in heart attacks and strokes. Therefore, patients with atherosclerosis should receive accurate diagnosis and timely therapeutic intervention. With the advancements in nanomedicine, researchers have proposed new research strategies and methods for atherosclerosis imaging. This paper summarizes some current research findings on the use of nanomaterials in diagnosing atherosclerosis and offers insights for optimizing the imaging applications of nanomaterials in the future.

Introduction

The prevalence of chronic diseases is increasing every year due to global population growth and changing lifestyles and social environments, which has an impact on local economies and health.^{1,2} More than 500 million people globally suffer from cardiovascular disease (CVD).³ Research has indicated that while the mortality rate of CVD has significantly decreased in developed nations like the UK and the prevalence has not changed significantly over the past ten years, the burden of

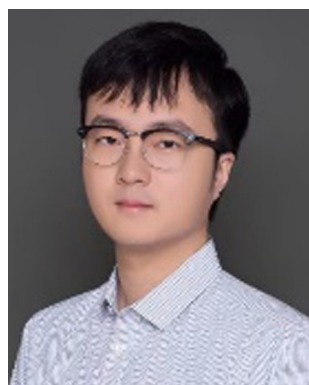
CVD is increasing in developing nations like China, India, and Africa, and countries still need to develop effective strategies to address the challenges posed by CVD.^{4–8}

Atherosclerosis is one of the major contributors to the development and progression of CVD. The global prevalence of atherosclerotic cardiovascular disease (ASCVD) has nearly quadrupled in the past 30 years, highlighting the tight association between ASCVD and CVD.⁹ The pathology of atherosclerosis is characterized by the formation of plaques and narrowing of blood vessels, where unstable plaques are prone to rupture and hemorrhage, from which intra-plaque material (*e.g.*, cholesterol crystals and inflammatory factors) enters the bloodstream and thrombus formation occurs, thereby partially or completely blocking the arteries and decreasing or blocking the blood supply to the heart, leading to unstable angina or myocardial infarction.⁹ Atherosclerosis can also cause a loss in artery flexibility, which can cause an increase in blood pressure, further harming the heart and blood vessels and eventually leading to major cardiovascular events.^{10,11} Thus, the prevention of CVD depends on the early detection and treatment of atherosclerosis.

Nanomaterials are substances with nano-size particles, and they are now widely employed in industrial, medicine, energy and environmental fields, among others. Nanomedicine is an interdisciplinary research field; a large number of novel nanomaterials are used in research on diagnosis and treatment of diseases, which offers multiple advantages in the field of medical science, such as targeting, retention effects, excellent physicochemical properties, biocompatibility and so on.^{12,13} The diagnosis of diseases is of great clinical significance, and researchers have shown that nanomaterials have considerable potential to be utilized as probes for biomedical imaging due to

^a Academy of Medical Sciences, Tianjian Laboratory of Advanced Biomedical Sciences, Zhengzhou University, Zhengzhou, Henan, China.
E-mail: weijiang@zzu.edu.cn

^b Department of pharmacy, Central China Subcenter of National Center for Cardiovascular Diseases, Henan Cardiovascular Disease Center, Fuwai Central-China Cardiovascular Hospital, Central China Fuwai Hospital of Zhengzhou University, Zhengzhou 450046, China. E-mail: lydyzjj@163.com



Wei Jiang

Wei Jiang is a principal investigator at the Academy of Medical Sciences, Tianjian Laboratory of Advanced Biomedical Sciences of Zhengzhou University. He obtained his PhD degree from Jilin University in 2018. His research focuses on the biological applications of nanozymes. He currently serves as an academic editor for *Exploration*.

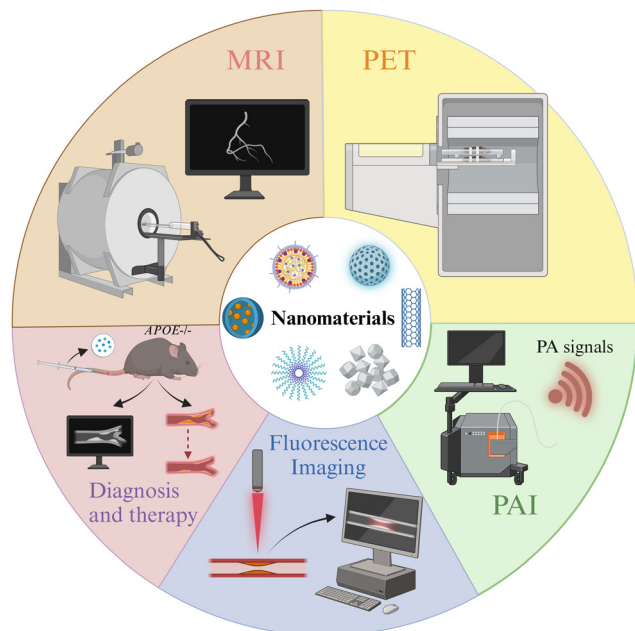


Fig. 1 Schematic diagram of the review: nanoparticles with different capabilities for imaging and treatment of atherosclerosis. Created with <https://BioRender.com>.

their advantages of targeted, real-time and dynamic imaging, high contrast, and multifunctionality for application in imaging techniques such as magnetic resonance imaging (MRI), computed tomography (CT), and optical imaging, among others.¹⁴ Combining nanoparticles with specific ligands, antibodies, or biomembranes enhances the specific recognition of atherosclerosis by targeting and identifying early stages of the disease. Nanotechnology offers the advantage of multifunctionality, allowing nanoparticles with both diagnostic

and therapeutic functions to facilitate drug delivery and imaging. Nanomaterials are easily designed and optimized in terms of size, shape, and properties, offering customization potential for precision medical treatment in the future.¹⁵ This review focuses on the construction of nanoparticles with applications in imaging and diagnosing atherosclerosis (Fig. 1).

1. Characteristics of atherosclerosis and the importance of its diagnosis

The development of atherosclerosis is a complex process involving various risk factors and pathological changes. A comprehensive understanding of the characteristics of atherosclerosis and its pathological changes can help researchers to develop imaging and therapeutic strategies for this disease.

1.1. Characteristics and pathological changes of atherosclerosis

Hyperlipidemia, hypertension, aging, obesity, diabetes mellitus, and the body's inflammatory environment all increase the risk of developing atherosclerosis, which is characterized by plaque formation and hardening of the blood arteries (Fig. 2A). It has been investigated that the lower the patient's adherence to managing hypertension, the higher the level of cardiovascular disease risk factors, and the risk of cardiovascular disease grows with age.¹⁶

Various stimuli such as hypertension, smoking, and hyperlipidemia can induce varying levels of damage to endothelial cells. This leads to adherence of molecules like low-density lipoproteins (LDLs) and platelets to these dysfunctional cells. Additionally, damaged endothelial cells release cytokines, promoting monocyte aggregation and adhesion. The monocytes then migrate to the interstitial space of the endothelial cells



Fig. 2 Schematic diagram of atherosclerosis characteristics and pathological changes. (A) Vascular features of atherosclerosis. (B) Pathological changes of atherosclerosis. Created with <https://BioRender.com>.

through chemotaxis, differentiate into macrophages, and ingest oxidized lipids beneath the endothelial membrane *via* scavenger receptors on their surface, resulting in the formation of macrophage-derived foam cells. Moreover, smooth muscle cells (SMCs) absorb lipids through lipoprotein lipase (LPL) receptors, forming SMC-derived foam cells. The accumulation of foam cells contributes to the development of lipid plaques in atherosclerosis (Fig. 2B).^{17–20} Overall, atherosclerosis is a progressive pathological process involving endothelial cell damage, LDL oxidation, inflammation, monocyte migration, and smooth muscle cell proliferation, which affect the systemic vasculature and a variety of organs throughout the body, *e.g.*, affecting the health of hematopoietic stem and progenitor cells in the bone marrow, decreasing their regenerative capacity, affecting lymphatic vascularity and function, and leading to myocardial infarction and stroke.^{21,22}

1.2. The importance of atherosclerosis diagnosis

By analyzing the autopsy reports of young people between 15 and 34 years of age, it was found that early lesions (*e.g.*, fatty streaks) and typical lesions of atherosclerosis already existed in young individuals, which suggests that the development of atherosclerosis is a long-term process and that its onset and early stages occur at a young age, implying that we need to begin to pay attention to and manage cardiovascular health at an earlier age in order to reduce the risk of cardiovascular disease in the future, and also puts a higher demand on diagnostic technologies with higher sensitivity and specificity for atherosclerosis, which will assist physicians in detecting the disease in its early stages more quickly and accurately.²³

Nanotechnology can enable targeted imaging of atherosclerotic lesions based on pathological changes. For instance, targeted ligands or modified cell membranes can be used to specifically detect key cells (such as macrophages and monocytes) and lesion-specific markers (*e.g.*, integrin $\alpha_v\beta_3$) involved in the atherosclerosis process. Additionally, the environmental features at the site of an atherosclerotic lesion, such as lipids, ROS, and inflammation, can be utilized for precise lesion identification. Furthermore, nanomaterials can passively target the abnormal vascular permeability in the lesion area due to their size advantage.²⁴ Nanotechnology can enhance the detection of atherosclerosis through the aforementioned strategies.

2. The rise of imaging nanomaterials

Nanomaterials are rapidly developing, boosting the advancement of a variety of fields. Nanomedicine has emerged as an important step in the development of modern medicine, with applications including cancer imaging and treatment and treatment of CVD, renal illness, and more, providing novel ideas for disease diagnosis and treatment.

2.1. Traditional imaging techniques

Imaging technology plays an important role in disease diagnosis, risk assessment, and treatment monitoring. Currently, invasive coronary angiography (ICA), computed tomography

angiography (CTA), magnetic resonance angiography (MRA), positron emission tomography (PET), intravascular ultrasound (IVUS), optical coherence tomography (OCT), and near-infrared (NIR) imaging are the main diagnostic techniques used for the diagnosis of atherosclerosis in clinical settings, but the above techniques have their advantages and limitations.^{25,26} ICA is the gold standard for the diagnosis of coronary artery disease (CAD), but it is invasive; radiation and contrast media have an impact on the body, and it is difficult to identify diffuse stenosis. CTA has high spatial resolution and is less invasive, but it has a clear requirement for the heart rate and takes time to process the images. MRI does not have radiation and does not require contrast media, but it has a longer imaging duration, is susceptible to motion, and in the case of complex and irregular blood flow, signal loss may result in the failure to identify the details of the pathology.²⁷ PET offers high sensitivity and can be combined with complementary imaging modalities like computed tomography (CT) and magnetic resonance imaging (MRI); however, it suffers from poor spatial resolution and can cause interference with myocardial uptake.²⁸ IVUS enables high-resolution imaging and analysis of plaque composition. However, it suffers from invasiveness and costliness, along with the potential of calcified plaques to obstruct ultrasound penetration.²⁹ OCT offers the benefits of non-invasiveness, rapid scanning speed, high resolution, and the ability to detect atherosclerotic plaque characteristics; however, it comes with a high cost and demands a relatively high skill level from operators.³⁰ NIR imaging offers the advantage of noninvasiveness and can complement the structural information obtained from ICA, IVUS, and OCT. Nonetheless, IR imaging still presents limitations in terms of imaging depth and susceptibility to interference from blood or biomolecules. Further validation of NIR imaging in clinical settings is warranted.^{31,32}

2.2. The rise of nanotechnology

The size, shape and potential of nanomaterials can be controlled during the synthesis process; the surface modification of nanomaterials by target molecules, probe markers, or drugs can be used for precision imaging and therapy to achieve high biocompatibility, laying the foundation for medical research.^{33,34} The properties listed above offer new diagnostic strategies and considerable potential for the application of nanomaterials in medicine. Nanomaterials for imaging are now being explored, showing promising results in CVD, cancer, liver illnesses, and brain diseases and providing new options for future disease diagnosis.^{35–39} Among them, magnetic nanoparticles have become a very promising research and application direction in the field of magnetically guided bioimaging,⁴⁰ and organic nanoparticles with near-infrared absorption capacity have been applied in photoacoustic imaging to successfully improve imaging quality and treatment efficiency.⁴¹

Compared with traditional imaging materials, nanomaterials with imaging capabilities have the advantages of multifunctionality, dynamic monitoring, and realization of interdisciplinary cooperation and can realize precise diagnosis of atherosclerotic

diseases and bring innovations in the diagnosis and treatment of atherosclerosis by identifying and imaging plaques or inflammatory macrophages through their specific targeting capabilities.⁴²

3. Imaging nanomaterials for atherosclerosis

With the rapid development of nanomaterials, some nanomaterials with MRI, PET, PAI and other capabilities have been successfully constructed and applied in the study of atherosclerotic diseases to provide new strategies for precise imaging and treatment of the diseases. This review summarizes and briefly describes the following research results (Table 1).

3.1. Nanomaterials with MRI capability

As a non-invasive, radiation-free imaging method for the diagnosis of cardiovascular illness, MRI uses magnetic fields and radio waves to examine the internal structures of the human body. In MRI, T1- and T2-weighted imaging modes are two commonly used imaging modes, with T1 imaging displaying structural features of tissues and T2 imaging identifying tissue abnormalities such as lesions and edema, and a key measure of contrast media performance is the relaxation rate (r_1).⁵⁹ Nanomaterials containing magnetic elements such as gadolinium (Gd) and iron (Fe) are commonly used as MRI contrast media for research due to their unique physical and chemical properties.

Ziyue Zu *et al.*⁴³ synthesized RpMPs by first preparing ultra-small-sized nanoparticles (MNPs) using the natural polyphenol melanin and then performing targeted functionalization with polyethylene glycol (PEG) and a cyclic-Arg-Gly-Asp-D-Tyr-Lys (cRGD) peptide. After incubation at 40 °C for 4 h, Gd³⁺ could attach directly to MNPs or RpMPs without the need for additional chelators to synthesize Gd³⁺-RpMPs and the control Gd³⁺-NpMPs. The researchers confirmed the high targeting efficiency of RpMPs and showed enhanced signal enhancement by comparing the MRI results of Gd³⁺-RpMPs and control Gd-DTPA, a paramagnetic contrast media, or Gd³⁺-NpMPs. Lydia

Martínez-Parra *et al.*⁴⁴ prepared ultrasmall calcium carbonate nanoparticles containing gadolinium element, and alendronate (for microcalcification targeting) and trimannose (for inflammation targeting) were modified on the nanoparticles to construct CC-Aln and CC-Trm, respectively. Gd³⁺-doped amorphous calcium carbonate nanoparticles were used for imaging studies of atherosclerotic plaques, and the results showed that CC-Aln exhibited significant imaging signal enhancement with better lesion targeting (Fig. 3A). Lingyi Wen *et al.*⁴⁵ synthesized ultrasmall Zn_{0.4}Fe_{2.6}O₄ nanoparticles using dynamic simultaneous thermal decomposition (DSTD), which were synthesized by the use of three different ligands, namely, dopamine (DA), 3,4-dihydroxyhydrocinnamic acid (DHCA) and phosphorylated polyethylene glycol (PO-mPEG) to modulate the surface charge of the nanoparticles. Zn_{0.4}Fe_{2.6}O₄-NH₂, Zn_{0.4}Fe_{2.6}O₄-COOH, and Zn_{0.4}Fe_{2.6}O₄-PEG were finally synthesized with positive, negative and neutral surface charges, respectively. The results showed that Zn_{0.4}Fe_{2.6}O₄ nanoparticles with different surface charges had higher relaxation rates compared to Gd-DTPA, a commonly used clinical contrast medium. Attributed to the high affinity of positive charge for macrophages, Zn_{0.4}Fe_{2.6}O₄-NH₂ exhibited the highest signal intensity among the three nanoparticles, and plaque lesions could be clearly imaged in 10 minutes (Fig. 3B). Xin Huang *et al.*⁴⁶ synthesized Fe₃O₄ nanoparticles by solvothermal synthesis and coated the nanoparticles with a macrophage membrane (MM) to provide the ability to target early atherosclerotic lesions (foam cell formation) and successfully prepared Fe₃O₄@M as well as the control Fe₃O₄@PEG. The nanoparticles were spherical in shape, measuring roughly 300 nm, with a significant T2 effect and good biosafety. In rats with atherosclerosis, Fe₃O₄@M nanoparticles were injected through the tail vein, and the results showed significant MRI signals in the area of early atherosclerotic lesions in the aortic root, and the targeting of Fe₃O₄@M was confirmed by comparing Fe₃O₄@M with Fe₃O₄@PEG nanoparticles by immunohistochemistry (IHC), demonstrating the diagnostic potential of Fe₃O₄@M for early atherosclerotic lesions (Fig. 3C).

Table 1 Different functional nanoparticles for diagnostic imaging of atherosclerosis

| Year | Author | Nanoparticles | Target | Application | Ref. |
|------|------------------------------------|--|---|----------------------|------|
| 2023 | Ziyue Zu <i>et al.</i> | Gd ³⁺ -RpMPs | α _v β ₃ | MRI | 43 |
| 2023 | Lydia Martínez-Parra <i>et al.</i> | CC-Aln/CC-Trm | Microcalcification/macrophages | MRI | 44 |
| 2024 | Lingyi Wen <i>et al.</i> | Zn _{0.4} Fe _{2.6} O ₄ Nps | Macrophages | MRI | 45 |
| 2021 | Xin Huang <i>et al.</i> | Fe ₃ O ₄ @M | Macrophages | MRI | 46 |
| 2017 | Edmund J. Keliher <i>et al.</i> | ¹⁸ F-Macroflor | Macrophages | PET/CT | 47 |
| 2019 | Hyeon Jin Jeong <i>et al.</i> | DBCO-MSNs | Macrophages | PET | 48 |
| 2016 | Carlos Pérez-Medina <i>et al.</i> | ⁸⁹ Zr-AI-HDL/ ⁸⁹ Zr-PL-HDL | Macrophages and monocytes | PET | 49 |
| 2016 | Hannah P. Luehmann <i>et al.</i> | ⁶⁴ Cu-vMIP-II-comb | Chemokine receptors | PET | 50 |
| 2021 | Mahsa Gifani <i>et al.</i> | SWNT-Cy5.5 | Ly-6C ^{hi} monocytes and foamy macrophages | PAI | 51 |
| 2023 | Yuan Ma <i>et al.</i> | L-CRP | Lipophilic environments and cathepsin B | PAI | 52 |
| 2023 | Jun Lu <i>et al.</i> | PCN@FL | HClO and phosphorylation | Fluorescence imaging | 53 |
| 2023 | Di Ma <i>et al.</i> | MeOTTI-PMEA NPs | Acidic environment | Fluorescence imaging | 54 |
| 2021 | Mangmang Sang <i>et al.</i> | CN-PD | — | Fluorescence imaging | 55 |
| 2018 | Wen Gao <i>et al.</i> | CuS-TRPV1 | — | PAI | 56 |
| 2024 | Qiao Chen <i>et al.</i> | pep-CDs | Foam cells | PAI | 57 |
| 2020 | Guanghao Wu <i>et al.</i> | MNC@M-ST/AP | Macrophages | MRI | 58 |



Fig. 3 Synthesis process and imaging application of MRI-enabled nanoparticles: (A) CC-Aln and CC-Trm nanoparticles. Copyright 2023 American Chemical Society. (B) Ultrasmall $Zn_{0.4}Fe_{2.6}O_4$ nanoparticles. Copyright 2024 American Chemical Society. (C) $Fe_3O_4@M$ nanoparticles. Copyright 2021 Elsevier.

In summary, nanomaterials combined with MRI technology have exhibited excellent imaging capabilities, providing more ideas for the development of novel MRI clinical application strategies in the future.

3.2. Nanomaterials with PET capability

PET is a nuclear medicine imaging technique that relies on the physical properties of positron-emitting nuclides.⁶⁰ In particular, radioisotope labeling, such as ^{18}F labelling, is a commonly used radiolabeling approach that is applied to PET imaging techniques when combined with biomolecules or compounds.

Edmund J. Keliher *et al.*⁴⁷ prepared ultra-small size (5.0 ± 0.4 nm) polyglucose nanoparticles (Macroflor), which were rendered PET imaging capable by ^{18}F labeling, and the nanomaterials showed both macrophage-targeting ability and rapid metabolism from the kidneys due to their small size and the polyglucose structure's macrophage-attracting properties. Experimental results showed that Macroflor nanoparticles achieved rapid renal excretion in three different species (mice, rabbits, and primates), and in mice and rabbits suffering from atherosclerosis, PET/CT imaging succeeded in ^{18}F -labeled Macroflor-specific enrichment in the aortic root and arch regions (Fig. 4A). Hyeon Jin Jeong *et al.*⁴⁸ constructed nanomaterials of

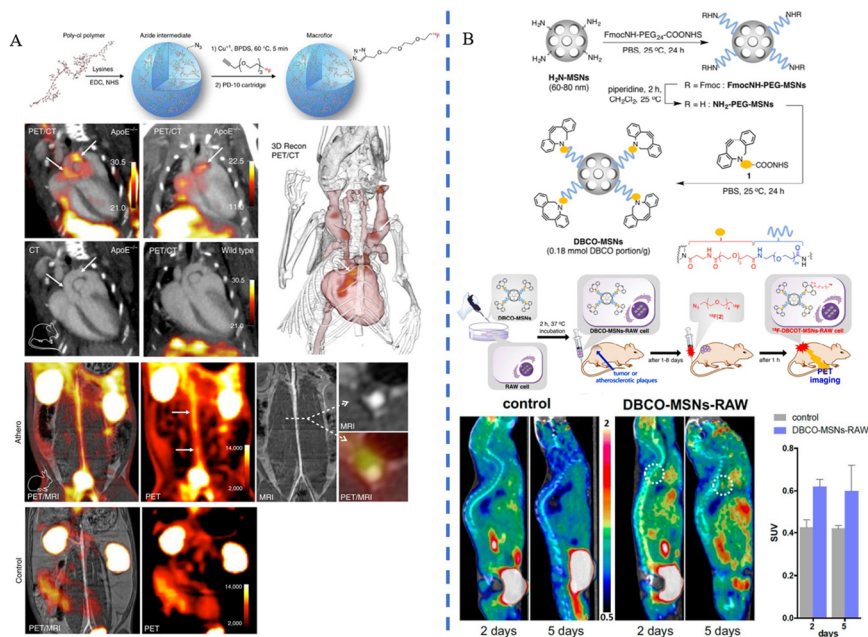


Fig. 4 Synthesis process and imaging applications of PET-enabled nanoparticles (A) ^{18}F -Macroflor nanoparticles. Copyright 2017, The Author(s). (B) DBCO-MSN nanoparticles. Copyright 2019 Elsevier.

DBCO-MSNs (polyethylene glycolized mesoporous silica nanoparticles with azodibenzocyclooctyne), and injected DBCO-MSNs-RAW into mice following macrophage phagocytosis. The researchers synthesized the radiolabeled precursor [^{18}F] fluoropentaethylene glycolic azide ([^{18}F]2) containing ^{18}F and an azido group in advance, and injected it into the animals; the azido group and the intracellular DBCO group underwent strain-promoted azide-alkyne cycloaddition (SPAAC) reaction. This reaction was a bioorthogonal reaction, meaning that it did not interfere with the organism's own biochemical reactions, thus ensuring labeling specificity. The researchers performed PET imaging in animal models of tumors and atherosclerosis, respectively. Through *in vivo* ^{18}F labeling, the researchers were able to effectively track and image the distribution and dynamics of macrophages in tumors and atherosclerotic plaques, which is expected to lead to early diagnosis of the diseases (Fig. 4B). Carlos Pérez-Medina *et al.*⁴⁹ synthesized disc-shaped high-density lipoprotein (HDL) nanoparticles by reconstructing the components, labeled the nanoparticles with ^{89}Zr -oxalate as a radioisotope source *via* chelator deferoxamine B conjugation or phospholipid-chelator binding, and constructed ^{89}Zr -apolipoprotein A-I labeled HDL (^{89}Zr -AI-HDL) and ^{89}Zr -phospholipid-labeled HDL (^{89}Zr -PL-HDL) to realize PET imaging function, respectively. The results showed that the blood half-life of ^{89}Zr -AI-HDL in mice ranged from 1.4 to 2.0 h, while that of ^{89}Zr -PL-HDL ranged from 1.1 to 2.8 h. In mouse and rabbit animal models, both HDL nanoparticles could achieve the targeting of macrophages and monocytes in the plaques, and the biodistribution of ^{89}Zr -HDL nanoparticles was observed by PET imaging, especially in the plaque accumulation in lesions. Hannah P. Luehmann *et al.*⁵⁰ first synthesized comb-shaped nanoparticles with amphiphilicity, attached viral macrophage inflammatory protein-II (vMIP-II) and then conjugated the ^{64}Cu radioisotope to form vMIP-II-conjugated nanoparticles, ultimately constructing the stabilized radiolabeled complex ^{64}Cu -vMIP-II-comb nanoparticles. The results showed that the retention time of ^{64}Cu -vMIP-II-comb nanoparticles in the blood was significantly increased compared to ^{64}Cu -comb, and PET imaging in mice modeled for vascular damage and atherosclerosis showed that ^{64}Cu -vMIP-II-comb nanoparticles displayed targeted imaging and a better imaging degree than ^{64}Cu -comb.

In summary, use of nanoparticles provides a promising research method for PET imaging.

3.3. Nanomaterials with photoacoustic imaging (PAI) capability

The principle of PAI, a rapidly emerging biomedical multi-wave imaging technique, is that the electromagnetic wave energy of the light absorber is absorbed by the biological tissues and transformed into thermal energy. The absorber body then expands and contracts thermally to become an acoustic source, and signal processing creates a photoacoustic image that reflects the structure and function of the tissue.⁶¹

Mahsa Gifani *et al.*⁵¹ prepared single-walled carbon nanotubes (SWNTs), which were able to be selectively taken up by

inflammatory Ly-6C^{hi} monocytes and foam cells, and were used for imaging after coupling with the fluorescent dye Cy5.5 (SWNT-Cy5.5). The nanotubes' ability to be specifically enriched in the lesion plaque allowed them to absorb light energy and convert it into heat when exposed to light. This caused the local temperature to increase as the nanotubes appeared to expand thermally, leading to minute vibrations and producing ultrasonic signals that were picked up by the detector and translated into images, fulfilling the goal of imaging the lesion. The breakdown of the fibrous cap by Cathepsin B (CTB) is an important factor causing the instability of plaques. Yuan Ma *et al.*⁵² combined lipophilic alkyl chains and hydrophilic CTB substrates onto hemicyanine scaffolds, using lipids and CTB as two "keys" to unlock photoacoustic (PA) signaling, and finally succeeded in constructing an L-CRP probe. In lipid-rich environments, such as foam cells in plaque regions, lipophilic alkyl chains enabled hemicyanine scaffolds to disperse and transform into monomers, ultimately realizing an increase in light absorption, which resulted in a stronger signal when irradiated with laser light. When the laser pulse activated the L-CRP probe, it caused thermal expansion of the surrounding tissue and then this thermal expansion generated sound waves, which subsequently propagate to the surface of the tissue. In animal experiments, L-CRP was able to dynamically report intra-plaque CTB levels and closely correlate with the characteristics of vulnerable plaques, enabling risk stratification of model mice for atherosclerosis. In addition, in isolated human artery tissues, the L-CRP probe was able to distinguish between atheromatous and normal vessels, implying that L-CRP could be used in clinical practice to help diagnose vulnerable plaques (Fig. 5).

PAI, due to its non-invasive nature and low cost compared to advanced imaging techniques, combines with nanomaterials to provide targeted and thus more accurate imaging, thus providing new strategies for early diagnosis of diseases.

3.4. Nanomaterials with fluorescence imaging capability

Fluorescence imaging is a technique that utilizes fluorescent probes to perform imaging at specific wavelengths of excitation light, which has the advantages of being non-invasive and sensitive, *etc.* However, conventional fluorophores are prone to aggregation-induced bursts and background fluorescence interference. As a solution, researchers have developed nanomaterials that incorporate fluorescent probes capable of extending their cycling time. These nanomaterials offer versatility, targeting capabilities, and precise imaging characteristics. They can be effectively used for precise imaging and treatment at various stages of atherosclerosis due to their unique optical properties.^{62,63}

Jun Lu *et al.*⁵³ synthesized PCN-224, a metal-organic framework containing Zr(IV), and TCFL, a small-molecule fluorescent probe containing fluorescein and dimethylthiocarbamate (DMTC), and then combined the two parts to successfully build PCN@FL with fluorescence imaging function. Hypochlorous acid (HClO) and phosphorylation are involved in the process of atherosclerosis. The selective recognition of the levels of HClO



Fig. 5 Synthesis process and PAI of L-CRP nanoparticles. (A) Schematic diagram of the L-CRP nanoparticle imaging process. (B) Design of animal experiments. (C) Probing the imaging effect of L-CRP in atherosclerosis model mice. (D) Exploring the imaging function of L-CRP in human artery samples. Copyright 2023 American Chemical Society.

and phosphorylation was achieved by the specific interaction between DMTC and HClO and the interaction between Zr(IV) and phosphate. The fluorescence imaging investigations revealed that PCN@FL is a useful fluorescence tool for assessing early atherosclerosis (Fig. 6A). Di Ma *et al.*⁵⁴ developed a fluorescent probe MeOTTI with specific aggregation-induced emission (AIE) properties, loaded with tetraphenylethylene (TPE) derivatives, which emits strong fluorescence signals in non-polar environments, such as lipid droplets, or in an aggregated state, and then encapsulated this probe into pH responsive polymer micelles to construct MeOTTI-PMEA NPs, which improved the water solubility and biocompatibility of

MeOTTI and enabled rapid release of MeOTTI in acidic environments such as lysosomes in cells. The experimental results demonstrated that the probe could successfully label lipid droplets for imaging atherosclerotic lesions (Fig. 6B). Mangmang Sang *et al.*⁵⁵ designed a lipid droplet-specific fluorescent probe (CN-PD) that achieves rapid intraoperative plaque imaging by atomizing an aqueous solution of CN-PD into 3-micrometer-sized microdroplets and then spraying them *in situ* on the lesion site, which can be utilized for rapid intraoperative determination of the lesion area and can provide a new idea for precise clinical treatment (Fig. 6C).



Fig. 6 Synthesis process and imaging applications of fluorescence imaging nanoparticles. (A) PCN@FL nanoparticles. Copyright 2023 John Wiley and Sons. (B) MeOTTI-PMEA nanoparticles. Copyright 2023 Elsevier. (C) CN-PD nanoparticles. Copyright 2021 American Chemical Society.

3.5. Nanomaterials for diagnosis and treatment

Researchers have employed nanomaterials to combine imaging and therapeutic capabilities, creating novel approaches for clinical atherosclerosis applications.

Transient Receptor Potential Vanilloid 1 (TRPV1), also known as the capsaicin receptor or vanilloid receptor, is a heat-sensitive cation channel. Wen Gao *et al.*⁵⁶ successfully constructed CuS-TRPV1 by combining CuS nanoparticles with a monoclonal antibody against TRPV1. Using near-infrared laser irradiation, CuS-TRPV1 was able to cause a localized increase in temperature on the surface of vascular smooth muscle cells, which resulted in activation of the TRPV1 channel, leading to the influx of calcium ions into the cells, activation of the AMPK signaling pathway, an increase in cholesterol efflux, and a decrease in lipid accumulation in the cells. Visualization of blood vessels by photoacoustic imaging and real-time monitoring of the therapeutic effect on atherosclerosis are shown in Fig. 7A. A nanozyme is a new type of nanomaterial that has the ability to mimic natural enzymes. Qiao Chen *et al.*⁵⁷ synthesized a carbon-dot nanozyme (pep-CDs) with involvement of the phosphatidylserine (PS)-specific peptide CLIKKPF. The pep-CD nanozyme had superoxide dismutase (SOD)-like enzyme activity and could play an anti-oxidative stress role; the CDs could absorb light energy and convert it into acoustic energy in response to PAI, thus generating signals in PAI; the specific recognition of CLIKKPF with PS on the outer surface of foam cell membranes endowed the nanozyme with targeting ability. As a new type of nanozyme, pep-CDs could not only effectively diagnose atherosclerosis through PAI, but also realize the treatment of atherosclerosis through its antioxidant and anti-inflammatory effects (Fig. 7B). Guanghao Wu *et al.*⁵⁸ used Fe₃O₄

magnetic nanoclusters (MNCs) with MRI imaging capabilities as the core, wrapped the MNCs in macrophage membranes *via* electrostatic adsorption to provide the ability to target plaques, and then embedded the anti-inflammatory drug simvastatin (ST) and targeting apolipoprotein A-I mimetic 4F peptide (AP) on the membranes to construct MNC@M-ST/AP. The results demonstrated that MNC@M-ST/AP could effectively target early AS plaques, which showed high signals in MRI imaging and a considerable reduction in the AS plaque area (Fig. 7C).

Nanomaterials possessing diagnostic and therapeutic properties exhibit multifunctional characteristics, holding significant promise for enabling real-time disease monitoring and advancing early detection and precise treatment of atherosclerosis. However, they also encounter challenges related to biocompatibility and immunogenicity, necessitating additional research and optimization.

4. Summary and outlook

Since the introduction of nanotechnology, it has been widely used in various fields after its cross-fertilization with different disciplines. Researchers used the advantages of nanomaterials such as easy modification and small size to design nanomaterials with different characteristics, which successfully improved the efficiency and accuracy of imaging, realized the integration of atherosclerosis imaging and diagnosis, and provided new ideas for the development of novel diagnostic modalities for the disease.⁶⁴ This paper mainly summarizes the success of nanomaterials with different imaging capabilities in imaging plaque lesions at the animal level, and it is believed that in the future, researchers will continue to explore how to further improve the



Fig. 7 Synthesis, imaging and therapeutic processes of nanoparticles. (A) CuS-TRPV1 nanoparticles. Copyright 2018 The Author(s). (B) pep-CD nanozyme. Copyright 2023 Wiley-VCH GmbH. (C) MNC@M-ST/AP nanoparticles. Copyright 2020 Elsevier.

specific distribution, precise imaging, and rapid metabolism of nanoprobe *in vivo* by altering the physicochemical properties of the nanoprobe (*e.g.*, size, shape, surface charge, *etc.*) and optimizing the synthesis methods, among other strategies.

New therapeutic strategies offer promise for improving clinical diagnosis and treatment. Although progress is being made in the clinical translation of nanomedicines, the current translation rate remains low.⁶⁵ The safety of nanomedicines *in vivo* poses a significant challenge to their clinical translation. Other factors include biological barriers *in vivo* that restrict nanomedicine efficacy, low reproducibility in nanomedicine preparation, challenges in achieving mass production, inadequate regulatory policies, and limited public acceptance of nanomaterials, all of which hinder their clinical translation.^{66–68} Therefore, future research should explore more multimodal imaging techniques to achieve a more comprehensive analysis of the plaques; studies need to further determine the distribution and metabolism pathways of nanomaterials and to further clarify the mechanism of nanomaterials to achieve *in vivo* imaging and treatment; in the future, the biocompatibility and degradability of nanomaterials need to be further improved to ensure their safety *in vivo*; and diagnostic strategies for the asymptomatic period of the disease need to be continuously developed to gain more time for interventional therapy. In the future, regulatory bodies should establish clinical translational regulations and guidelines to support the advancement of nanomaterials. Furthermore, researchers are encouraged to enhance the reproducibility and production yields of nanomaterials through optimization of preparation methods.^{69,70} The world is currently experiencing a rapid period of clinical research on nanomedicines, with emerging technologies being continuously updated. Challenges and opportunities are interwoven, and it is anticipated that more nanomedicines will be utilized in clinical settings in the future.

In summary, nanotechnology has great potential for research and translational applications in the diagnosis and treatment of atherosclerosis. It is expected to develop new approaches for clinical diagnosis and treatment, to achieve a more comprehensive assessment of the disease and provide patients with more clinical options.

Author contributions

Ying Yang was responsible for writing the manuscript. Wei Jiang conceived the idea for this review. All authors contributed sections and provided feedback on each other's work. The submitted version was approved by all authors, who accepted responsibility for the work's content.

Data availability

No primary research results, software or codes have been included and no new data have been generated or analyzed as part of this review.

Conflicts of interest

There are no conflicts to declare.

Acknowledgements

The authors are grateful to the many scientists whose research findings have been mentioned here. This work was supported by the Young Elite Scientists Sponsorship Program by Henan Association for Science and Technology (Grant 2024HYTP048), Natural Science Foundation of Henan Province (No. 222300420573), and Henan Province Medical Science and Technology Tackling Program Joint Co-Construction Project (LHGJ20230129).

Notes and references

- 1 W. H. Dietz, C. E. Douglas and R. C. Brownson, *JAMA*, 2016, **316**, 1645–1646.
- 2 K. E. Thorpe and M. Philyaw, *Annu. Rev. Public Health*, 2012, **33**, 409–423.
- 3 G. A. Roth, G. A. Mensah, C. O. Johnson, G. Addolorato, E. Ammirati, L. M. Baddour, N. C. Barengo, A. Z. Beaton, E. J. Benjamin, C. P. Benziger, A. Bonny, M. Brauer, M. Brodmann, T. J. Cahill, J. Carapetis, A. L. Catapano, S. S. Chugh, L. T. Cooper, J. Coresh, M. Criqui, N. DeCleene, K. A. Eagle, S. Emmons-Bell, V. L. Feigin, J. Fernández-Solà, G. Fowkes, E. Gakidou, S. M. Grundy, F. J. He, G. Howard, F. Hu, L. Inker, G. Karthikeyan, N. Kassebaum, W. Koroshetz, C. Lavie, D. Lloyd-Jones, H. S. Lu, A. Mirijello, A. M. Temesgen, A. Mokdad, A. E. Moran, P. Muntner, J. Narula, B. Neal, M. Ntsekhe, G. Moraes de Oliveira, C. Otto, M. Owolabi, M. Pratt, S. Rajagopalan, M. Reitsma, A. L. P. Ribeiro, N. Rigotti, A. Rodgers, C. Sable, S. Shakil, K. Sliwa-Hahnle, B. Stark, J. Sundström, P. Timpel, I. M. Tleyjeh, M. Valgimigli, T. Vos, P. K. Whelton, M. Yacoub, L. Zuhlke, C. Murray and V. Fuster, GBD-NHLBI-JACC Global Burden of Cardiovascular Diseases Writing Group, *J. Am. Coll. Cardiol.*, 2020, **76**, 2982–3021.
- 4 P. Bhatnagar, K. Wickramasinghe, E. Wilkins and N. Townsend, *Heart*, 2016, **102**, 1945–1952.
- 5 P. B. Duell, V. Mehta, D. Nair, S. Puri, R. Nanda and R. Puri, *J. Clin. Lipidol.*, 2020, **14**, 170–172.
- 6 P. W. Wilson and B. F. Culleton, *Am. J. Kidney Dis.*, 1998, **32**, S56–S65.
- 7 D. Ahadzi, B. Gaye and Y. Commodore-Mensah, *Global Heart*, 2023, **18**, 20.
- 8 T. Wang, Z. Zhao, X. Yu, T. Zeng, M. Xu, Y. Xu, R. Hu, G. Chen, Q. Su, Y. Mu, L. Chen, X. Tang, L. Yan, G. Qin, Q. Wan, Z. Gao, G. Wang, F. Shen, Z. Luo, Y. Qin, L. Chen, Y. Huo, Q. Li, Z. Ye, Y. Zhang, C. Liu, Y. Wang, S. Wu, T. Yang, H. Deng, J. Zhao, Y. Xu, M. Li, Y. Chen, S. Wang, G. Ning, Y. Bi, L. Shi, J. Lu and W. Wang, *Lancet Regional Health – Western Pacific*, 2021, **17**, 100277.
- 9 K. Morton, B. Heindl, S. Clarkson and V. Bittner, *J. Cardiopulm. Rehabil. Prev.*, 2022, **42**, 389.

- 10 E. Gianazza, M. Brioschi, A. M. Fernandez and C. Banfi, *Redox Biol.*, 2019, **23**, 101119.
- 11 K. K. Poppe, S. Wells, R. Jackson, R. N. Doughty and A. J. Kerr, *Eur. J. Prev. Cardiol.*, 2021, **28**, 2010–2017.
- 12 T. Lammers and M. Ferrari, *Nano Today*, 2020, **31**, 100853.
- 13 M. Chang, C. Dong, H. Huang, L. Ding, W. Feng and Y. Chen, *Adv. Funct. Mater.*, 2022, **32**, 2204791.
- 14 D. Kim, J. Kim, Y. I. Park, N. Lee and T. Hyeon, *ACS Cent. Sci.*, 2018, **4**, 324–336.
- 15 S. Wang, H. He, Y. Mao, Y. Zhang and N. Gu, *Adv. Sci.*, 2024, **11**, 2308298.
- 16 L. Xiaoling, H. Tian, C. Yang, G. Wu and N. Jia, *J. Am. Coll. Cardiol.*, 2016, **68**, C70.
- 17 E. Mousseaux, L. Agoston-Coldea, Z. Marjanovic, R. Stanciu, C. Deligny, L. Perdrix, P. Boutouyrie, A. Azarine, G. Soulat and D. Farge, *J. Am. Coll. Cardiol.*, 2018, **71**, 703–705.
- 18 D. E. Gutstein and V. Fuster, *Cardiovasc. Res.*, 1999, **41**, 323–333.
- 19 Y. Asada, A. Yamashita, Y. Sato and K. Hatakeyama, *Pathol. Int.*, 2020, **70**, 309–322.
- 20 Y. Baumer, N. N. Mehta, A. K. Dey, T. M. Powell-Wiley and W. A. Boisvert, *Eur. Heart J.*, 2020, **41**, 2236–2239.
- 21 W. C. Keeter, S. Ma, N. Stahr, A. K. Moriarty and E. V. Galkina, *Semin. Immunopathol.*, 2022, **44**, 363–374.
- 22 A. Zmysłowski and A. Szterk, *Lipids Health Dis.*, 2017, **16**, 188.
- 23 C. A. McMahan, S. S. Gidding, G. T. Malcom, R. E. Tracy, J. P. Strong and J. McGill Henry, *Pediatrics*, 2006, **118**, 1447–1455.
- 24 J. Wang, B. Lu, G. Yin, L. Liu, P. Yang, N. Huang and A. Zhao, *ACS Biomater. Sci. Eng.*, 2024, **10**, 1190–1206.
- 25 M. R. Dweck, E. Aikawa, D. E. Newby, J. M. Tarkin, J. H. F. Rudd, J. Narula and Z. A. Fayad, *Circ. Res.*, 2016, **119**, 330–340.
- 26 E. A. Osborn, C. W. Kessinger, A. Tawakol and F. A. Jaffer, *J. Nucl. Med.*, 2017, **58**, 871–877.
- 27 L. E. Mantella, K. Liblik and A. M. Johri, *Atherosclerosis*, 2021, **319**, 42–50.
- 28 P. Joseph and A. Tawakol, *Eur. Heart J.*, 2016, **37**, 2974–2980.
- 29 H. M. Garcia-Garcia, M. A. Costa and P. W. Serruys, *Eur. Heart J.*, 2010, **31**, 2456–2469.
- 30 R. Takeshige, H. Otake, H. Kawamori, T. Toba, Y. Nagano, Y. Tsukiyama, K. Yanaka, H. Yamamoto, A. Nagasawa, H. Onishi, Y. Sugizaki, S. Nakano, Y. Matsuoka, K. Tanimura and K. Hirata, *Heart Vessels*, 2022, **37**, 1–11.
- 31 S. Sanon, T. Dao, V. P. Sanon and R. Chilton, *Curr. Atheroscler. Rep.*, 2013, **15**, 304.
- 32 X. Luo, J. Shi, R. Wang, L. Cao, Y. Gao, J. Wang, M. Hong, X. Sun and Y. Zhang, *ACS Nano*, 2024, **18**, 6500–6512.
- 33 J. Pellico, P. J. Gawne and R. T. M. de Rosales, *Chem. Soc. Rev.*, 2021, **50**, 3355–3423.
- 34 J. Ouyang, A. Xie, J. Zhou, R. Liu, L. Wang, H. Liu, N. Kong and W. Tao, *Chem. Soc. Rev.*, 2022, **51**, 4996–5041.
- 35 S. Shi, F. Chen, S. Goel, S. A. Graves, H. Luo, C. P. Theuer, J. W. Engle and W. Cai, *Nano-Micro Lett.*, 2018, **10**, 65.
- 36 L. H. Reddy and P. Couvreur, *J. Hepatol.*, 2011, **55**, 1461–1466.
- 37 F. Liang, Q. You, X. Ma, H. Wang, C. Wang, Z. He, Y. Yang and L. Zhu, *Nano Res.*, 2023, **16**, 13134–13163.
- 38 X. Hu, Z. Chen, A. J. Jin, Z. Yang, D. Gan, A. Wu, H. Ao, W. Huang and Q. Fan, *Small*, 2021, **17**, 2007566.
- 39 M. Zhang, Z. Xie, H. Long, K. Ren, L. Hou, Y. Wang, X. Xu, W. Lei, Z. Yang, S. Ahmed, H. Zhang and G. Zhao, *Mater. Today Bio*, 2022, **14**, 100236.
- 40 J. Mohapatra, S. Nigam, J. George, A. C. Arellano, P. Wang and J. P. Liu, *Mater. Today Phys.*, 2023, **32**, 101003.
- 41 Y. Jiang and K. Pu, *Small*, 2017, **13**, 1700710.
- 42 W. J. M. Mulder, F. A. Jaffer, Z. A. Fayad and M. Nahrendorf, *Sci. Transl. Med.*, 2014, **6**, 239sr1–239sr1.
- 43 Z. Zu, J. Sheng, J. Qi, Y. Miao, Y. Zhang, T. Zheng, K. Xiang, H. Wu, G. Lu and L. Zhang, *Adv. Funct. Mater.*, 2023, **33**, 2212748.
- 44 L. Martínez-Parra, M. Piñol-Cancer, C. Sanchez-Cano, A. B. Miguel-Coello, D. Di Silvio, A. M. Gomez, C. Uriel, S. Plaza-García, M. Gallego, R. Pazos, H. Groult, M. Jeannin, K. Geraki, L. Fernández-Méndez, A. Urkola-Arsuaga, M. J. Sánchez-Guisado, J. Carrillo-Romero, W. J. Parak, M. Prato, F. Herranz, J. Ruiz-Cabello and S. Carregal-Romero, *ACS Nano*, 2023, **17**, 13811–13825.
- 45 L. Wen, X. Fu, H. Zhang, P. Ye, H. Fu, Z. Zhou, R. Sun, T. Xu, C. Fu, C. Zhu, Y. Guo and H. Fan, *ACS Appl. Mater. Interfaces*, 2024, **16**, 13496–13508.
- 46 X. Huang, C. Lin, C. Luo, Y. Guo, J. Li, Y. Wang, J. Xu, Y. Zhang, H. Wang, Z. Liu and B. Chen, *Nanomedicine*, 2021, **33**, 102348.
- 47 E. J. Keliher, Y.-X. Ye, G. R. Wojtkiewicz, A. D. Aguirre, B. Tricot, M. L. Senders, H. Groenen, F. Fay, C. Perez-Medina, C. Calcagno, G. Carlucci, T. Reiner, Y. Sun, G. Courties, Y. Iwamoto, H.-Y. Kim, C. Wang, J. W. Chen, F. K. Swirski, H.-Y. Wey, J. Hooker, Z. A. Fayad, W. J. M. Mulder, R. Weissleder and M. Nahrendorf, *Nat. Commun.*, 2017, **8**, 14064.
- 48 H. J. Jeong, R. J. Yoo, J. K. Kim, M. H. Kim, S. H. Park, H. Kim, J. W. Lim, S. H. Do, K. C. Lee, Y. J. Lee and D. W. Kim, *Biomaterials*, 2019, **199**, 32–39.
- 49 C. Pérez-Medina, T. Binderup, M. E. Lobatto, J. Tang, C. Calcagno, L. Giesen, C. H. Wessel, J. Witjes, S. Ishino, S. Baxter, Y. Zhao, S. Ramachandran, M. Eldib, B. L. Sánchez-Gaytán, P. M. Robson, J. Bini, J. F. Granada, K. M. Fish, E. S. G. Stroes, R. Duivenvoorden, S. Tsimikas, J. S. Lewis, T. Reiner, V. Fuster, A. Kjær, E. A. Fisher, Z. A. Fayad and W. J. M. Mulder, *JACC: Cardiovasc. Imaging*, 2016, **9**, 950–961.
- 50 H. P. Luehmann, L. Detering, B. P. Fors, E. D. Pressly, P. K. Woodard, G. J. Randolph, R. J. Gropler, C. J. Hawker and Y. Liu, *J. Nucl. Med.*, 2016, **57**, 1124.
- 51 M. Gifani, D. J. Eddins, H. Kosuge, Y. Zhang, S. L. A. Paluri, T. Larson, N. Leeper, L. A. Herzenberg, S. S. Gambhir, M. V. McConnell, E. E. B. Ghosn and B. R. Smith, *Adv. Funct. Mater.*, 2021, **31**, 2101005.
- 52 Y. Ma, J. Shang, L. Liu, M. Li, X. Xu, H. Cao, L. Xu, W. Sun, G. Song and X.-B. Zhang, *J. Am. Chem. Soc.*, 2023, **145**, 17881–17891.

- 53 J. Lu, Z. Li, M. Lu, N. Fan, W. Zhang, P. Li, Y. Tang, X. Yin, W. Zhang, H. Wang and B. Tang, *Adv. Mater.*, 2023, **35**, 2307008.
- 54 D. Ma, W. Zhuang, Q. Liu, J. Chen, C. Li, S. Li and M. Chen, *Chem. Eng. J.*, 2023, **476**, 146792.
- 55 M. Sang, B. Cai, S. Qin, S. Zhao, Y. Mao, Y. Wang, X. Yu and J. Zheng, *ACS Appl. Mater. Interfaces*, 2021, **13**, 58369–58381.
- 56 W. Gao, Y. Sun, M. Cai, Y. Zhao, W. Cao, Z. Liu, G. Cui and B. Tang, *Nat. Commun.*, 2018, **9**, 231.
- 57 Q. Chen, X. Duan, Y. Yu, R. Ni, G. Song, X. Yang, L. Zhu, Y. Zhong, K. Zhang, K. Qu, X. Qin and W. Wu, *Adv. Sci.*, 2024, **11**, 2307441.
- 58 G. Wu, W. Wei, J. Zhang, W. Nie, L. Yuan, Y. Huang, L. Zuo, L. Huang, X. Xi and H.-Y. Xie, *Biomaterials*, 2020, **250**, 119963.
- 59 V. Grover, J. Tognarelli, M. Crossey, I. Cox, S. Taylor-Robinson and M. McPhail, *J. Clin. Exp. Hepatol.*, 2015, **5**, 246–255.
- 60 A. Rahmim, M. A. Lodge, N. A. Karakatsanis, V. Y. Panin, Y. Zhou, A. McMillan, S. Cho, H. Zaidi, M. E. Casey and R. L. Wahl, *Eur. J. Nucl. Med. Mol. Imaging*, 2019, **46**, 501–518.
- 61 A. Zare, P. Shamshiripour, S. Lotfi, M. Shahin, V. F. Rad, A.-R. Moradi, F. Hajiahmadi and D. Ahmadvand, *J. Controlled Release*, 2022, **351**, 805–833.
- 62 Z. Guo and Z. Cui, *Wiley Interdiscip. Rev.: Nanomed. Nanobiotechnol.*, 2021, **13**, e1705.
- 63 C. Li, G. Chen, Y. Zhang, F. Wu and Q. Wang, *J. Am. Chem. Soc.*, 2020, **142**, 14789–14804.
- 64 R. Qiao, H. Qiao, Y. Zhang, Y. Wang, C. Chi, J. Tian, L. Zhang, F. Cao and M. Gao, *ACS Nano*, 2017, **11**, 1816–1825.
- 65 M. A. Younis, H. M. Tawfeek, A. A. H. Abdellatif, J. A. Abdel-Aleem and H. Harashima, *Adv. Drug Delivery Rev.*, 2022, **181**, 114083.
- 66 Y. Liu, Z. Jiang, X. Yang, Y. Wang, B. Yang and Q. Fu, *Adv. Healthcare Mater.*, 2024, **13**, 2303612.
- 67 P. Yang, J. Ren and L. Yang, *Int. J. Mol. Sci.*, 2023, **24**, 5205.
- 68 H. Omidian, N. Babanejad and L. X. Cubeddu, *Pharmaceutics*, 2023, **15**, 1935.
- 69 X. Li, C. Wang, H. Tan, L. Cheng, G. Liu, Y. Yang, Y. Zhao, Y. Zhang, Y. Li, C. Zhang, Y. Xiu, D. Cheng and H. Shi, *Biomaterials*, 2016, **108**, 71–80.
- 70 K. Wang, H. Gao, Y. Zhang, H. Yan, J. Si, X. Mi, S. Xia, X. Feng, D. Liu, D. Kong, T. Wang and D. Ding, *Adv. Mater.*, 2022, **34**, 2106994.